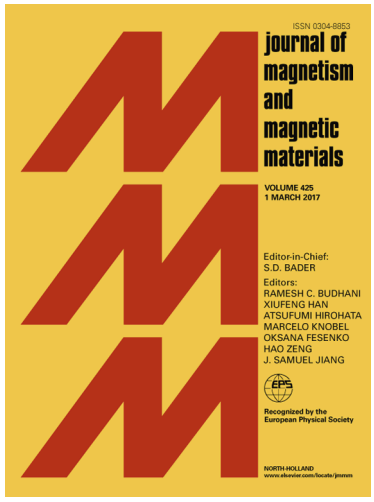

Magnetic Phase Coexistence in $DyNiAl_4$

R. White, W.D. Hutchison, M. Avdeev

PII: S0304-8853(17)33836-2
DOI: https://doi.org/10.1016/j.jmmm.2018.08.011
Reference: MAGMA 64208

To appear in: *Journal of Magnetism and Magnetic Materials*

Received Date: 29 January 2018
Revised Date: 5 August 2018
Accepted Date: 5 August 2018

Please cite this article as: R. White, W.D. Hutchison, M. Avdeev, Magnetic Phase Coexistence in $DyNiAl_4$, *Journal of Magnetism and Magnetic Materials* (2018), doi: https://doi.org/10.1016/j.jmmm.2018.08.011

Magnetic Phase Coexistence in $DyNiAl_4$

R. White[a], W.D. Hutchison[a] and M. Avdeev[b]

[a] *School of Physical, Environmental and Mathematical Sciences, The University of New South Wales, Canberra ACT 2600, Australia.*
[b] *Australian Centre for Neutron Scattering, Australian Nuclear Science and Technology Organisation, Kirrawee DC NSW 2232, Australia.*

Abstract
The magnetic structure and properties of the rare earth intermetallic $DyNiAl_4$ have been determined. Two magnetic phase transitions have been observed at T_N = 20.2(1) K and $T_{N'}$ = 14.6(1) K. Analysis via neutron diffraction has revealed that these correspond to the formation of two distinct magnetic phases, a low temperature collinear antiferromagnetic phase with $\boldsymbol{k_C}$ = (0,1,0) and a higher temperature incommensurate phase with $\boldsymbol{k_I}$ = (0.1745(6), 1, 0.0313(6)). The incommensurate phase consists of a sinusoidal modulation of the magnetic moment along the *a*- and *c*-axis directions. In addition, both of these phases have been found to coexist between 14.5 K and 16.1 K.

Keywords: Rare earth intermetallics, neutron powder diffraction, incommensurate magnetic phase

1. Introduction

The $RNiAl_4$ ($R = Ln^{3+}$) series has shown a remarkable variety of magnetic properties and structures all dependent on the particular rare earth ion present within the compound [1-10]. All have the *$YNiAl_4$* structure type and belong to the *Cmcm* space group and common to all members of the series thus far studied is an incommensurate magnetic phase, with the exact configuration of the moments varying between different ions. For example, in $TbNiAl_4$ the incommensurate magnetic structure consists of an elliptical helix type structure with the moments rotating close to the *ab*-plane while moving along the *c*-axis [1-3]. In $PrNiAl_4$, the structure consists of a sinusoidally modulated moment along the *a*-axis, the same direction in which the moments point [4]. In both of these cases, the magnetic structure transitions to commensurate antiferromagnetism once the temperature is low enough [1, 5]. In contrast the magnetic structures of $ErNiAl_4$ [6] and $NdNiAl_4$ [7, 8] remain incommensurate to the lowest measured temperatures. This suggests that Kramer's degeneracy may play a role in the number of phase transitions a series member may have. $DyNiAl_4$ is a Kramer's ion but has been found previously to possess two phase transitions ($T_N \approx 18$ K and $T_{N'} \approx 15$ K) [9], behaviour only seen thus far amongst non-Kramer's ions of the $RNiAl_4$ series. New heat capacity and neutron diffraction measurements have been carried out on $DyNiAl_4$ in order to determine both the number and nature of its magnetic phases to compare and contrast with other compounds in the series, both Kramer's and non-Kramer's based.

2. Experimental

$DyNiAl_4$ was synthesised by combining stoichiometric amounts of the constituent elements (Dy 99.9%, Ni 99.99%, Al 99.999%) before melting in an argon arc furnace several times to ensure homogeneity. The buttons obtained were then wrapped in tantalum foil before being placed in an evacuated quartz tube and annealed for 1 week at 1030°C. Phase purity was checked via X-ray diffraction using a PANalytical Empyrean X-ray Diffractometer with Cu radiation. Heat capacity measurements were carried out using a Quantum Design Physical

Property Measurement System while neutron diffraction was performed using the *ECHIDNA* high resolution powder diffractometer [11] located at the OPAL Reactor, Lucas Heights, Sydney, Australia. The wavelength used was 2.4395 Å and diffraction patterns were refined using the *Fullprof* suite of programs [12]. The polycrystalline sample was contained within a 6 mm vanadium sample can using a Debye-Scherrer transmission geometry for the experiment. In order to account for the effect of high neutron absorption by the Dy within the sample, the absorption correction facility within Fullprof was used, with the value for μR set to -2.477. The process to arrive at this parameter started with a calculated value based on the sample geometry and chemical composition then optimised for the best refinement of the 40 K nuclear pattern. The negative value triggers Fullprof to invoke the Lobanov and Alte da Veiga model [13] which is recommended for higher absorption cases. The initial measurements were performed from base temperature up to 40 K, while a second run of measurements was done in the order of 16.5 K, 18.5 K and finally 14.5 K.

3. Results

3.1 Heat Capacity

Heat capacity measurements carried out on a 5.0 mg single solid piece of $DyNiAl_4$ are plotted in Figure 1. It is immediately apparent that there are two phase transitions, the first located at T_N = 20.2(1) K and the second at $T_{N'}$ = 14.6(1) K and these are much more well defined than those of the previous powder measurement [9]. Data of Figure 1a was collected with increasing steps however no temperature directional dependence of these transitions was found, as illustrated in Figure 1b which shows data for both step directions. Also included on Figure 1a is the scaled specific heat data for isostructural, non-magnetic $YNiAl_4$ which allows a quantification of the magnetic entropy of the $DyNiAl_4$ compound. Scaling was done using the many-Debye method [14] and the resulting magnetic entropy obtained from the difference of the two data sets is shown in Figure 2. At 60 K, the entropy curve appears be approaching saturation at a value of 13.0 J/mol K, well short of the expected value of 23.1 J/mol K determined using the relation $R\ln(2J+1)$ for Dy^{3+} with J = 15/2. Although a shortfall in this quantity may be expected due to crystal field effects, in this case it is more likely that the many-Debye approximation, based around a large mass scaling between Y and Dy has become less valid at higher temperatures. Instead, if we only use the value of the entropy up to just after T_N, we find that it reaches a value of 6.3 J/mol K and repeating the above analysis gives a value of $2J+1$ = 2.1 or roughly 2 levels contributing to the entropy, indicating that only the ground state doublet has significant population during the magnetic phase transitions. This corresponds well with the observation from inelastic neutron scattering data that there is a 6.5 meV (75.4 K) difference in energy from the ground state to the first excited state [10].

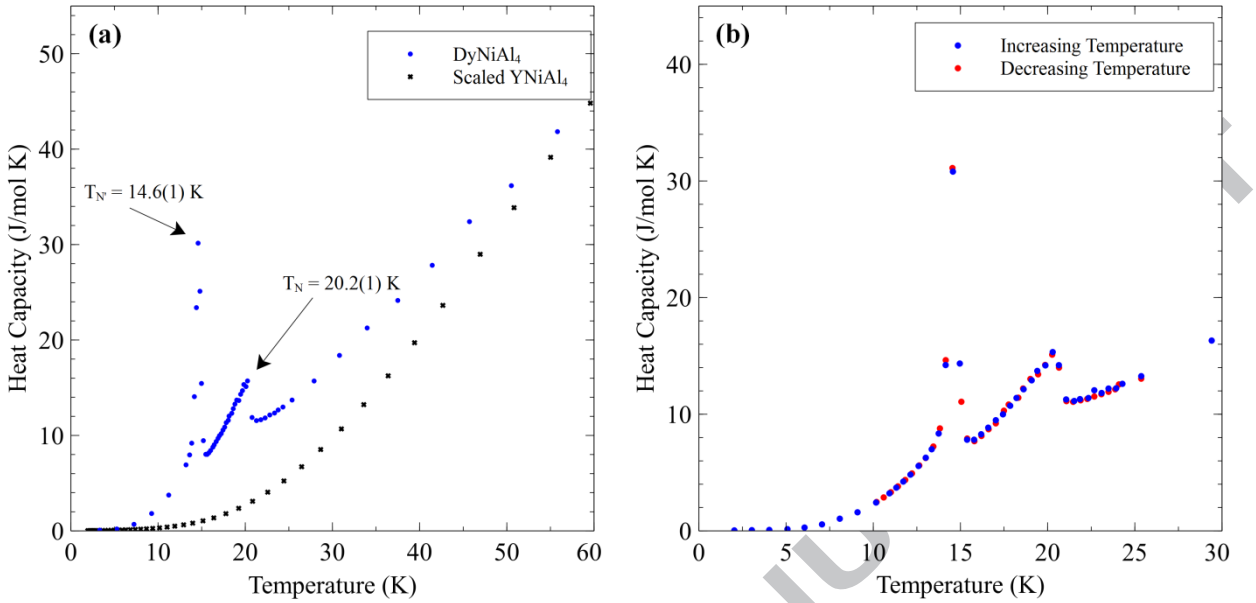

Figure 1: Heat capacity data obtained from a 5.0 mg solid offcut of $DyNiAl_4$ and the scaled heat capacity of $YNiAl_4$ are shown in (a). There are two magnetic transitions at 20.2(1) K and 14.6(1) K which correspond with an incommensurate and commensurate magnetic ordering respectively based on subsequent neutron diffraction experiments. In (b) the heat capacity around the transitions is shown with increasing and decreasing temperature.

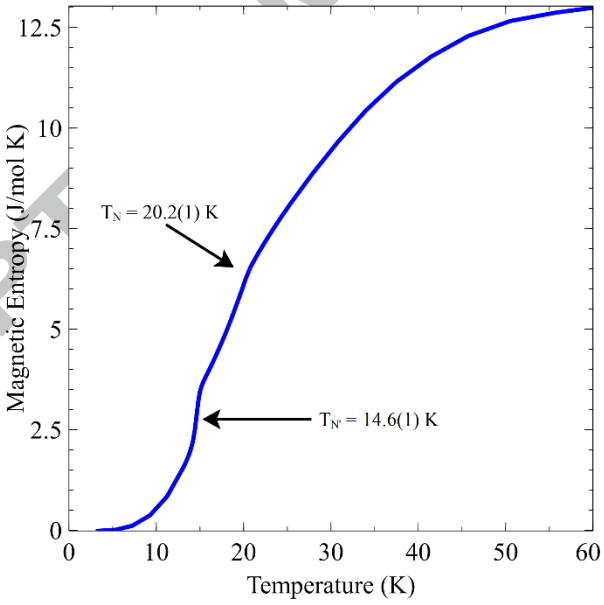

Figure 2: Magnetic entropy calculated for $DyNiAl_4$. At 60 K, the entropy reaches a value of 13.1 J/mol K which is well short of the expected 23.1 J/mol K for Rln(2J+1) with J = 15/2. At just above T_N the entropy is equal to 6.3 J/mol K which corresponds with only 2 crystal field levels being occupied (i.e. the ground state)

3.2 Neutron Diffraction

Figure 3 is the neutron diffraction pattern recorded at 40 K, well above both ordering temperatures. The pattern fits well to the expected reflections of the *Cmcm* space group and *$YNiAl_4$* structure type. Note that the patterns from the 1.6 K, 16.1 K and 40 K runs are affected by cryostat impurity peaks from 60.95° to 64.00°, 65.74° to 67.26° and 71.21° to

76.00°. These regions have been excluded from the refinements. The data of Figure 4 is the diffraction pattern recorded at the base temperature of 1.6 K, where in contrast to Figure 3 magnetic reflections are clearly present, with the large peak at 2θ = 9° particularly prominent. These magnetic reflections index to a propagation vector of $\boldsymbol{k}_C$ = (0,1,0), the same propagation vector as that found in the commensurate phases of $TbNiAl_4$ [1] and $PrNiAl_4$ [5]. Magnetic structures can be described using the irreducible representations of the crystallographic space group [15, 16]. This is achieved here using the program *BasIreps*, part of the *Fullprof* suite. The irreducible representations corresponding to the aforementioned propagation vector are shown in Table 1 with two magnetic sites at (x,y,z) and (x, -y, z + ½) with each described by a single basis vector. The best refinement is achieved by using the Γ_4 representation. This leads to a collinear antiferromagnetic configuration with the magnetic moment aligned with the *a*-axis, bearing striking similarities to its non-Kramer's ion counterparts. It reaches a value of 8.1(1) μ_B which is somewhat smaller than the full free ion moment of Dy^{3+} of 10 μ_B and comparatively smaller than that measured in $TbNiAl_4$ where single crystal saturated magnetisation and neutron diffraction gave 8.6 μ_B c.f. a Tb^{3+} free ion value of 9.0 μ_B [2]. Moreover it should be noted that previous ^{161}Dy Mossbauer experiments on this material show the moment to be fully stretched [10] and thus a moment close to the free ion value should be expected. Therefore the apparent reduction in moment suggested by the neutron refinement should be viewed with caution as it may simply be due to the inability precisely account for the effect on the magnetic scattering caused by the strong neutron absorption of Dy. The refinement statistics for the 1.6 K pattern are shown in Table 2 while the structure is shown in Figure 5.

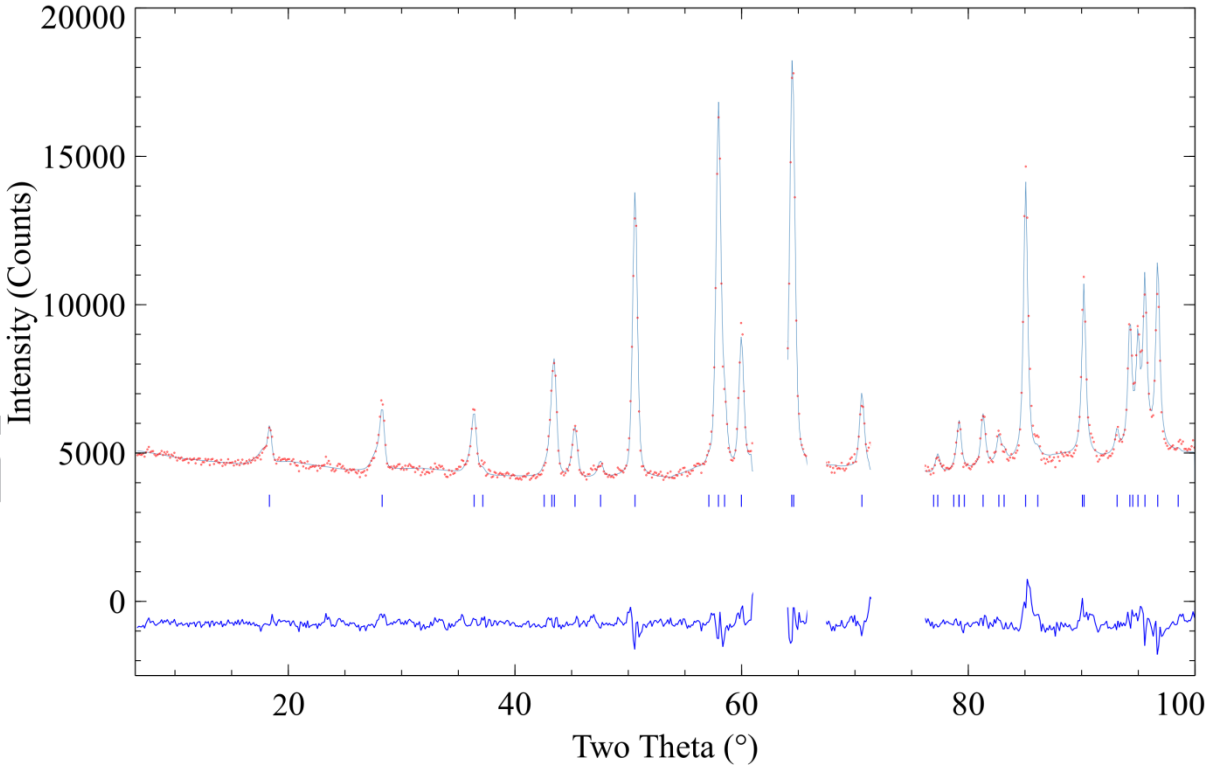

Figure 3: Refined neutron diffraction pattern of $DyNiAl_4$ taken at 40 K. As can be seen, the peaks that are present correspond well with the expected $YNiAl_4$ structure type and the Cmcm space group. Excluded regions are due to interference from the cryostat.

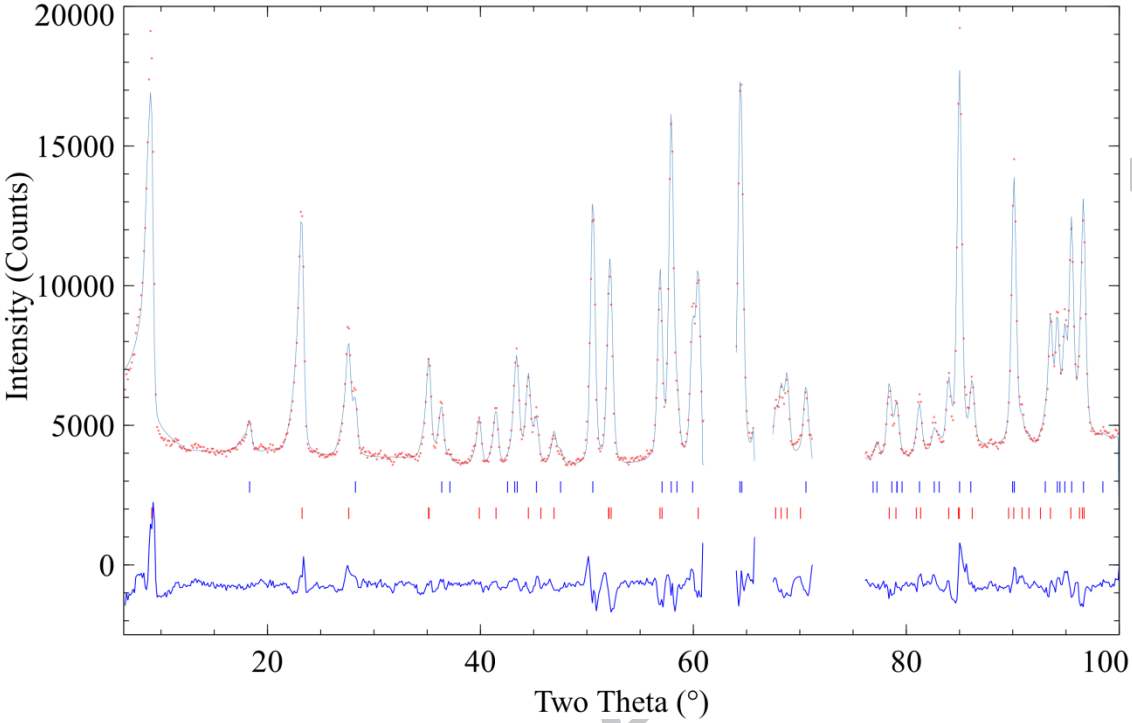

Figure 4: Refined neutron diffraction pattern of $DyNiAl_4$ taken at 1.6 K. Immediately apparent are the additional peaks when compared with the 40 K pattern. These correspond to a commensurate propagation vector of $\mathbf{k_c}$ = (0,1,0). The large magnetic moment on the Dy^{3+} ion provides numerous magnetic peaks allowing easy refinement of the magnetic structure. The blue (top) vertical lines correspond with nuclear reflections, while the red (bottom) lines correspond to magnetic reflections. Excluded regions are due to interference from the cryostat.

Irrep	**(x,y,z)**	**(x, -y, z + ½)**
Γ_2	(0, 1, 0)	(0, -1, 0)
Γ_3	(0, 0, 1)	(0, 0, 1)
Γ_4	(1, 0, 0)	(-1, 0, 0)
Γ_5	(0, 1, 0)	(0, 1, 0)
Γ_7	(1, 0, 0)	(1, 0, 0)
Γ_8	(0, 0, 1)	(0, 0, -1)

Table 1: Irreducible representations for $DyNiAl_4$ obtained using the propagation vector k_C = (0,1,0)

Atom	x	y	z
Dy (4c)	0	0.1193(4)	0.25
Ni (4c)	0	0.772(1)	0.25
Al1 (4b)	0	0.5	0
Al2 (4c)	0	0.929(4)	0.25
Al3 (8f)	0	0.312(3)	0.061(5)
k	0	1	0
***a* [Å]**		4.0421(2)	
***b* [Å]**		15.323(2)	
***c* [Å]**		6.5893(5)	
R_P [%]		12.1	
R_{wp} [%]		13.0	
R_{exp} [%]		4.01	
Bragg R-Factor [%]		3.75	
Mag R-Factor [%]		4.76	
Mag. Moment		8.1(1) μ_B	
χ^2		10.6	

Table 2: Refinement statistics and parameters for $DyNiAl_4$ (space group Cmcm) at 1.6 K

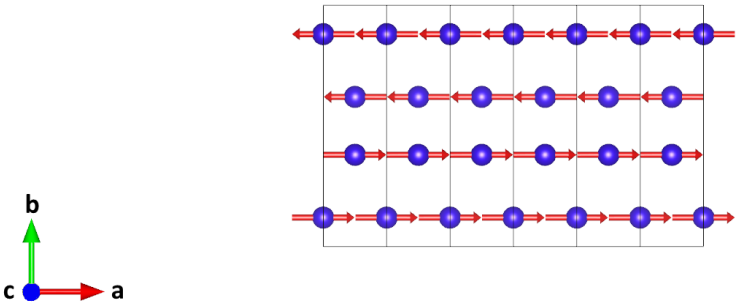

Figure 5: Magnetic structure of $DyNiAl_4$ at 1.6 K with propagation vector $\boldsymbol{k}_C$ = (0,1,0). Six unit cells along the a-axis are shown. It is identical to that found in the commensurate structures of $TbNiAl_4$ and $PrNiAl_4$. Atoms other than Dy have been excluded for clarity.

Figure 6 is the diffraction pattern measured at 16.1 K, well between the two transition temperatures. As can be seen, there is now a different magnetic phase present with the largest magnetic peaks no longer in the same position as they were previously. These peaks now index to the propagation vector $\boldsymbol{k}_I$ = (0.1745(6), 1, 0.0313(6)) which is reminiscent of all incommensurate propagation vectors found thus far in this series. This was determined using the propagation vector for $TbNiAl_4$ as a prototype and allowing the *h* and *l* components to refine. Based on this propagation vector, two irreducible representations (Γ_1 and Γ_2) are possible for $DyNiAl_4$ as shown in Table 3 and these include two magnetic sites at (x,y,z) and (x, -y, z + ½) described by the basis vectors shown. The first of these irreducible representations requires that the magnetic moments have parallel components along the *a* and *c*-axis directions while being antiparallel along the *b*-axis. The second is the opposite, with the moments antiparallel along the *a*- and *c*-axes but parallel along the *b*-axis. It was found that the best refinements were achieved using Γ_2 and indeed this matches with the magnetic structure determined at 1.6 K which had antiferromagnetic moment alignment along the *a*-axis.

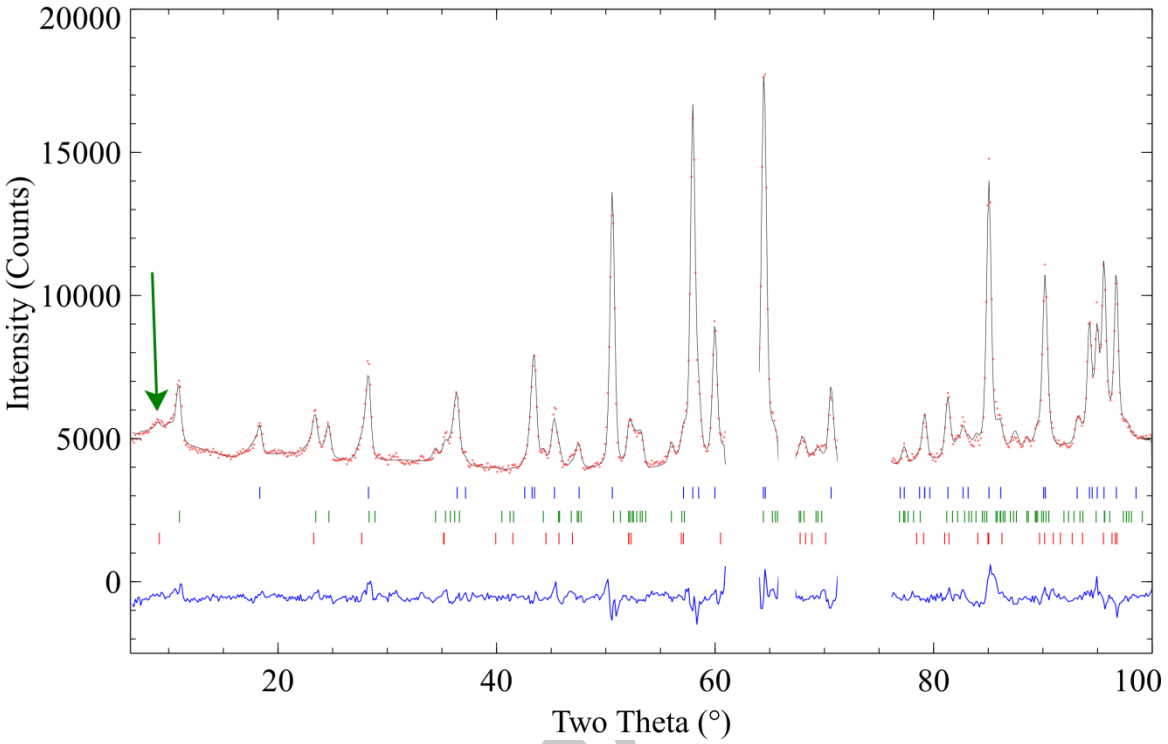

Figure 6: Refined neutron diffraction pattern for $DyNiAl_4$ at 16.1 K. The most intense magnetic peaks are now in different positions and these correspond to an incommensurate propagation vector with $\boldsymbol{k_I}$ = (0.1745(6), 1, 0.0313(6)). The location of another magnetic reflection that corresponds with the commensurate propagation vector $\boldsymbol{k_C}$ = (0,1,0) is indicated by the green arrow. The intensity of this peak is significantly reduced compared to that previously seen in the 1.6 K data and this appears to be the only reflection from that phase that is visible. The blue (top) vertical lines indicate nuclear reflections, green (middle) vertical lines indicate magnetic reflections from the incommensurate phase while the red (bottom) vertical lines indicate magnetic reflections from the commensurate phase. Excluded regions are due to interference from the cryostat.

$\boldsymbol{\Gamma_1}$	$\boldsymbol{\Gamma_2}$
(1,0,0) (1-0.10i, 0, 0)	(1,0,0) (-1+0.10i, 0, 0)
(0,1,0) (0, -1+0.10i, 0)	(0,1,0) (0, 1-0.10i, 0)
(0,0,1) (0,0,1-0.10i)	(0,0,1) (0, 0, -1+0.10i)

Table 3: Irreducible representations for $DyNiAl_4$ obtained using the propagation vector k = (0.1745(6), 1, 0.0313(6))

Overall, this irreducible representation corresponds to a magnetic structure in which the magnetic moments vary in magnitude along the *a*- and *c*-axis directions, similar to both $PrNiAl_4$ [4] and $ErNiAl_4$ [6] . A schematic of this magnetic structure over six unit cells is shown in Figure 7. More surprisingly however, the 16.1 K data appears to show remnants of the commensurate antiferromagnetic phase with the large peak at $2\theta = 9°$ still visible (indicated by the green arrow). It is also possible to fit the peak using the $\boldsymbol{k_C}$ = (0,1,0) commensurate propagation vector, as seen in Figure 6. The only other example of such phase coexistence in this series was observed in $TbNiAl_4$ with the aid of a magnetic field [2]. The phase evolution of the commensurate and incommensurate peaks across three more

temperatures: 14.5 K, 16.5 K and 18.5 K is detailed in Figure 8. As can be seen, the relative sizes of the peaks increase or decrease with temperature, indicating that the amount of each of the phases evolve with temperature.

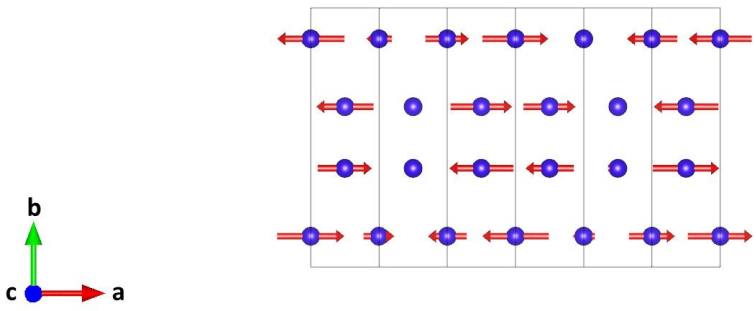

Figure 7: Incommensurate magnetic structure of $DyNiAl_4$ at 16.1 K and corresponding to propagation vector $\boldsymbol{k_I}$ = ((0.1745(6), 1, 0.0313(6)). Six unit cells along the a-axis are shown. There is sinusoidal modulation in the size of the magnetic moment along the easy (a) axis direction and this is also present along the c-axis, though is of a much greater periodicity as determined by the relatively small c-axis component of the propagation vector. Atoms other than Dy have been excluded for clarity.

In order to quantify the relative amounts of each phase present at a given temperature, the magnetic moments of the individual phases must be determined independently since both moment and phase fraction cannot be refined simultaneously. For the commensurate phase this can be achieved readily. The base temperature (1.6 K) magnetic moment of 8.1(1) μ_B as previously stated was scaled using the theoretical spontaneous magnetisation curve with $\boldsymbol{J}$ = 15/2 and an ordering temperature of T_N = 20.2 K. This results in a value for the moment of 4.7 μ_B at 16.1 K.

For the incommensurate structure, the moment amplitude was determined via a linear extrapolation from the 18.5 K and 16.5 K data sets which, as can be seen in Figure 8, contain no evidence of the commensurate phase. The maximum moment amplitude calculated for each temperature was 4.5(1) μ_B and 6.4(1) μ_B respectively. Extrapolating from these two values, we find the magnetic moment at 16.1 K to be 6.7 μ_B and at 14.5 K to be 8.2 μ_B. The moment size at 14.5 K has been set to the value that would be obtained at the phase transition of 14.6 K, as it is unlikely that there is any further increase in the size of the incommensurate magnetic moment below this temperature.

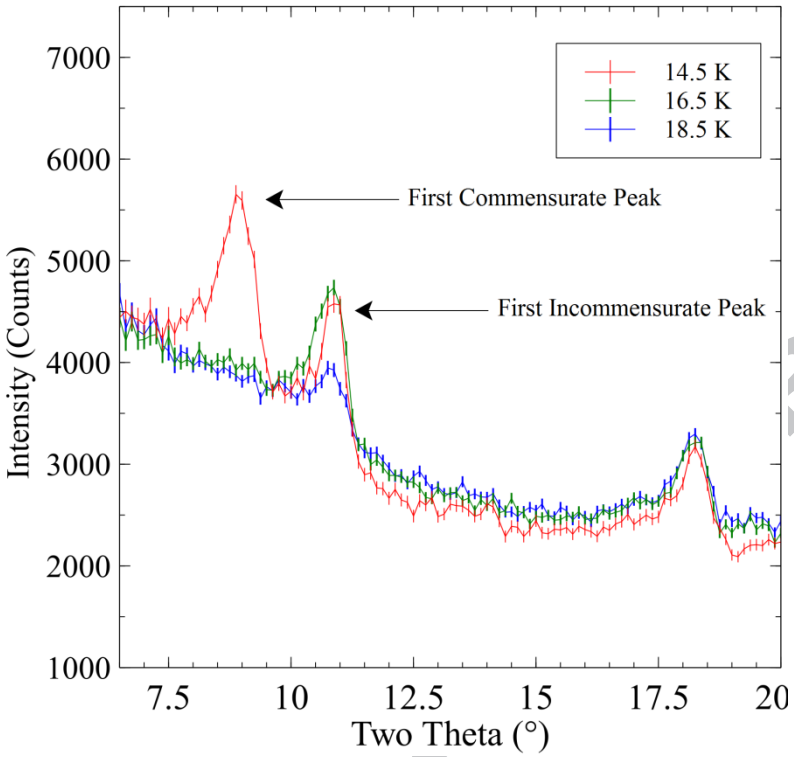

Figure 8: Magnetic peak variation of $DyNiAl_4$ at three different temperatures. As can be seen, at 18.5 K the only phase present is the incommensurate phase, with no evidence that a commensurate peak is present. Similarly at 16.5 K, where although there is a very slight rise in the intensity in the region where one would expect the commensurate peak to appear, its presence at this temperature appears to be minimal or non-existent. At 14.5 K the commensurate peak is well established and is now more intense than the incommensurate peak. When compared to the 16.1 K data (Figure 6, run with a different cryostat) the relative intensities of the two magnetic peaks have changed, indicating evolution of the amount of each magnetic phase. Note that the 14.5 K data has been scaled by a constant factor of 1.4 meaning no meaningful comparisons can be made between absolute heights, only relative heights within single patterns.

With these values determined the ratio of the magnetic phases to one another can be evaluated by fixing the sum of the two scale factors of the individual magnetic phases to the scale factor of the nuclear phase. Doing so reveals that only 7% of the material is in the commensurate phase at 16.1 K while the remaining 93% is incommensurately ordered. The refinement statistics and parameters for this fit are included in Table 4. At 14.5 K this ratio shifts to 43% commensurate and 57% incommensurate, indicating that even just below $T_{N'}$ there is still a majority amount of incommensurate phase present.

There is some evidence that the phase coexistence seen here in $DyNiAl_4$ is also present around the lower temperature magnetic transition in $TbNiAl_4$ [1]. However due to limitations of the original MRPD data, further experimental results are needed to verify this assertion beyond any doubt.

4. Conclusion

The structures of the two magnetic phases in $DyNiAl_4$ has been determined with transition temperatures of T_N = 20.2(1) K and $T_{N'}$ = 14.6(1) K. The two structures were found to consist of a lower temperature collinear antiferromagnetic phase with $\boldsymbol{k_C}$ = (0,1,0) and a higher temperature sinusoidally modulated incommensurate phase with $\boldsymbol{k_I}$ = (0.1745(6), 1, 0.0313(6)). These two magnetic phases are also found to coexist from 16.1 K down to at least

14.5 K with the relative heights of the magnetic peaks corresponding to each individual phase varying with temperature.

Atom	x	y	z
Dy (4c)	0	0.1180(4)	0.25
Ni (4c)	0	0.7720(8)	0.25
Al1 (4b)	0	0.5	0
Al2 (4c)	0	0.929(3)	0.25
Al3 (8f)	0	0.311(2)	0.061(4)
k_C	0	1	0
k_I	0.1745(6)	1	0.0313(6)
***a* [Å]**		4.0392(4)	
***b* [Å]**		15.312(1)	
***c* [Å]**		6.5865(4)	
R_P [%]		12.4	
R_{wp} [%]		11.9	
R_{exp} [%]		5.76	
Bragg R-Factor [%]		4.22	
Mag R-Factor (C/I) [%]		12.8/7.19	
Mag. Moment (C)		4.6 μ_B	
Mag. Amplitude (I)		6.7 μ_B	
χ^2		4.25	

Table 4: Refinement statistics and parameters for $DyNiAl_4$ (space group Cmcm) at 16.1 K. Note that there are two propagation vectors, k_C and k_I representing the commensurate and incommensurate structures respectively.

Acknowledgements
The authors wish to acknowledge the Australian Centre for Neutron Scattering for the allocation of beam time and AINSE for travel assistance. R. White acknowledges UNSW for scholarship support.

References

[1] Hutchison W D, Goossens D J, Nishimura K, Mori K, Isikawa Y and Studer A J 2006 *Journal of Magnetism and Magnetic Materials* **301** 352-358

[2] Hutchison W D, Goossens D J, Whitfield R E, Studer A J, Nishimura K and Mizushima T 2012 *Physical Review B* **86** 014412

[3] White R, Hutchison W D, Goossens D J, Studer A J and Nishimura K 2015 *Hyperfine Interactions* **231** 85-93

[4] White R, Hutchison W D, Avdeev M and Nishimura K 2016 *40th Annual CMM Meeting, (Wagga Wagga)*Australian Institute of Physics pp TP 15: 11 - 15

[5] Mizushima T, Isikawa Y, Sakurai J, Ohashi M and Yamaguchi Y 1997 *Journal of the Physical Society of Japan* **66** 3970-3974

[6] Stewart G A, Hutchison W D, Yamani Z, Cadogan J M and Ryan D H 2014 *38th Annual CMM Meeting, (Waiheke Island, New Zealand)*Australian Institute of Physics pp 24 - 27

[7] Mizushima T, Isikawa Y, Sakurai J, Mori K, Fukuhara T, Maezawa K, Schweizer J and Ressouche E 1994 *Physica B* **194** 225-226

[8] Tolinski T, Falkowski M, Synoradzki K, Hoser A and Stuesser N 2012 *Journal of Alloys and Compounds* **523** 43-48

[9] Hutchison W D, Segal N J and Nishimura K 2012 *36th Annual CMM Meeting, (Wagga Wagga)*Australian Institute of Physics pp WP14:11 - 14

[10] Hutchison W D, Stewart G A, Cadogan J M, Princep A, Stewart R and Ryan D H 2017 *AIP Advances* **7** 055702

[11] Liss K-D, Hunter B, Hagen M, Noakes T and Kennedy S 2006 *Physica B: Condensed Matter* **385–386, Part 2** 1010-1012

[12] Rodriguez-Carvajal J 1993 *Physica B* **192** 55-69

[13] Lobanov N N and Veiga L A d 1998 *Abstract, Sixth European Powder Diffraction Conference held in Budapest, Hungary* pp 12-16

[14] Bouvier M, Lethuillier P and Schmitt D 1991 *Physical Review B* **43** 13137-13144

[15] Rodríguez-Carvajal J and Bourée F 2012 *EPJ Web of Conferences* **22** 1 - 52

[16] Wills A 2001 *J. Phys. IV France* **11** 133-158

Highlights

- The magnetic structure and properties of $DyNiAl_4$ have been examined
- Two magnetic phases were found to exist
- A collinear antiferromagnetic phase exists below 16.1 K
- An incommensurate sinusoidally modulated phase exists below 20.2 K
- These two phases coexist between 16.1 K and 14.5 K